tion with polarization at 0.01 MHz. The five-layer model predicts about a 5:1 difference.

In conclusion, it is predicted theoretically that marked differences in tissue-absorbed power density can occur due to tissue anisotropy at frequencies below 10 MHz. Further research efforts on anisotropic effects must include more appropriate models. Whereas the model assumes infinitely long one-directional muscle fibers, actual skeletal muscle tissue contains finite fiber lengths. This is of little consequence in the model. In the legs and arms, muscle-fiber orientation is reasonably uniform and the one-directional model is useful. However, in other portions of the body skeletal muscle fibers are layered and run in several different directions. The model must be refined in these areas of the body. A finite-layered model such as an anisotropic sphere or spheroid is needed to extend the infinite-layered model results. The finite-model analysis is required before useful predictive quantitative data can be obtained. It has been previously demonstrated in this frequency range that body orientation with respect to the RF field vectors is an important factor in tissue-absorbed power density [4]. It is expected that body orientation combined with anisotropic effects will play a major role in effecting absorbed RF power density.

REFERENCES

[1] S. Rush, J. A. Abildskov, and R. McFee, "Resistivity of body tissues at low frequencies," *Circ. Res.*, vol. 12, pp. 40–50, Jan. 1963.
[2] H. P. Schwan, "Electrical properties of tissue and cell expansions," *Biol. Med. Phys.*, vol. 5, pp. 147–209, 1957.
[3] C. C. Johnson and A. W. Guy, "Nonionizing electromagnetic wave effects in biological materials and systems," *Proc. IEEE*, vol. 60, pp. 692–718, June 1972.
[4] C. H. Durney, C. C. Johnson, and H. Massoudi, "Long wavelength analysis of planewave electromagnetic power absorption by a prolate spheroidal tissue body," in *Proc. 1974 Annu. USNC-URSI Meeting* (Boulder, Colo., Oct. 1974), p. 110.

Fiber and Diffused Waveguide Structures for Distributed-Feedback Lasers

C. ELACHI, MEMBER, IEEE,
G. EVANS, STUDENT MEMBER, IEEE, AND
C. YEH, MEMBER, IEEE

***Abstract*—Optimum threshold conditions for oscillations of transversely bounded distributed-feedback (DFB) lasers are derived and discussed for the case of a fiber guide and diffused guide.**

The recent development of integrated-optics thin-film distributed-feedback (DFB) lasers [1]–[9] has generated much interest in the application of the DFB concept to other types of lasers. Basically, the DFB approach consists of replacing the two end mirrors by a volume or surface Bragg grating, throughout the active medium, which would provide enough feedback for self-sustained oscillation. Kogelnik and Shank [4] have analyzed in detail the properties of transversely unbounded DFB lasers. Elachi and Yeh [10] and Elachi *et al.* [11], have studied the case of a thin-film DFB laser and have shown that the presence of the transverse boundary has drastic effects on the feedback coupling and threshold gain. In this short paper, we derive the threshold conditions for fiber and diffuse DFB lasers, and we show that these structures are feasible with available active materials. A fiber DFB laser [Fig. 1(a)] can be used as a source of an optical-fiber communication channel and thus eliminate the input-coupling problem. A diffused-guide DFB laser [Fig. 1(d)] is attractive because it is easy to implement [12]. A gas-capillary laser with diffused cladding [Fig. 1(c)] has the advantage that it can support guided waves [13]. A diffuse guide has recently been developed [12] and analyzed [14]. Homogeneous-capillary DFB lasers were proposed by Marcuse [7].

Manuscript received May 6, 1974; revised January 17, 1975. This work was supported in part by NASA Contract NAS7-100, and in part by the Naval Electronics Laboratory Center.

C. Elachi and G. Evans are with the Jet Propulsion Laboratory, California Institute of Technology, Pasadena, Calif. 91103.
C. Yeh is with the Department of Engineering, University of California, Los Angeles, Calif. 90024.

If the boundary of an active waveguide is corrugated with a perturbation $\eta \cos(2\pi z/\Lambda)$, two contradirectional modes (p and q) are strongly coupled if they satisfy the Bragg condition

$$\beta_p + \beta_q = 2\pi/\Lambda \tag{1}$$

where β_i are the longitudinal wave vectors.

The coupling coefficient κ_{pq} [1], [15], [16], can be derived, in the case of small surface perturbation, by replacing the surface corrugation with a periodic surface current [11], [15], or by solving the exact boundary condition [10]. We found the coupling coefficient to be equal to

$$\kappa_{pq} = \eta \frac{\epsilon_1 - \epsilon_2}{2} k^2 (Q_p Q_q)^{-1/2} \tag{2}$$

where $k = \omega/c$ and Q_i are given in Table I for the fiber and diffuse guide case, and η is the amplitude of the periodic surface perturbation.

If one of the regions (inside or outside the guide) is an active medium with gain coefficient G, the effective gain coefficient would then be CG. This is due to the fact that the optical energy is never totally confined to the active region. The value of C was determined by taking the dielectric constant to be complex in the gain region and then solving for the (complex) longitudinal wave vector β_i. For small gain, a Taylor expansion series gives

$$C_i = \frac{k(\epsilon_1)^{1/2}}{\mathrm{Re}\{\beta_i\}} \frac{F_i}{1 + F_i} \tag{3}$$

for the case where the guiding region is active (inside the fiber or in the inhomogeneous half-space), and

$$C_i = \frac{k(\epsilon_2)^{1/2}}{\mathrm{Re}\{\beta_i\}} \frac{1}{1 + F_i} \tag{4}$$

for the case where the outside region is active (cladding or homogeneous half-space). The expression F is given in Table I. Independently, it can be shown that in the case of an active fiber the coefficient C_i is equal to

$$C_i = \frac{k(\epsilon_1)^{1/2}}{\mathrm{Re}\{\beta_i\}} \frac{P}{P + P'} \tag{5}$$

where P and P' are the powers inside and outside the fiber. The first term in (5) expresses the fact that the optical ray follows a zigzag line.

The threshold gain can now be determined by using a modified form [11] of the Kogelnik and Shank approach [4] to take into account the fact that the forward and backward waves could be different modes, and therefore might have different effective gains and group velocities.

The required threshold gain for laser oscillation is given by

$$G = \frac{2}{C_p(k) + C_q(k)} \mathrm{Re}\{Y_{pq}\} \tag{6}$$

and the corresponding phase mismatch by

$$\Delta k = \frac{2}{c(\psi_p(k) + \psi_q(k))} \mathrm{Im}\{Y_{pq}\} \tag{7}$$

where Y_{pq} is a solution of

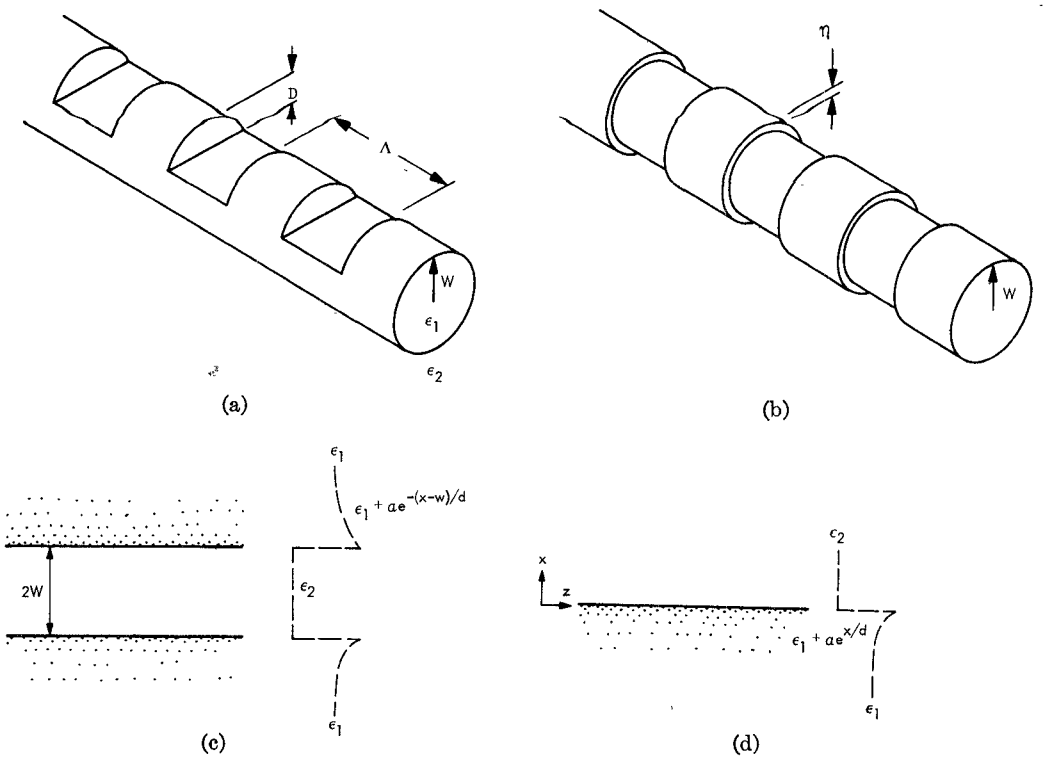

Fig. 1. DFB waveguide laser structures studied. (a) A DFB fiber laser. The corrugation can be generated by ion-beam machining. (b) An ideal DFB fiber laser which can be analyzed analytically. The relation between η and D can be derived using Fourier series expansion: $\eta = (D/\pi)(D/2w)^{1/2}$. (c) Diffuse DFB capillary laser. The inhomogeneity in the substrate allows waveguiding. (d) Diffuse DFB laser. The exponential change in the dielectric constant can be achieved with good approximation by diffusing foreign material in the lower half-space.

TABLE I

Configuration	Q	F
Fiber* [15]	$\frac{\beta}{\delta}\frac{J_0}{J_1}\left[sw\frac{K_1'}{K_1} + \delta w\frac{J_1'}{J_1} - \frac{s^2+\delta^2}{s\delta}\right]$	$-\frac{\delta}{s}\left[\frac{J_0/J_1 + sw\,(J_0/J_1)'}{K_0/K_1 + \delta w\,(K_0/K_1)'}\right]$
Diffuse [14]	$2\frac{\beta d}{\nu}\left\{\left(1+\frac{\nu}{2\delta d}\right)\left(1+2\delta d\frac{\partial J_\nu/\partial\nu}{J_\nu}\right) - 2kd\sqrt{\alpha}\frac{\partial J_{\nu+1}/\partial\nu}{J_\nu}\right.$	$\frac{2\sqrt{\alpha}\,kd\,\delta d}{\nu}\frac{\partial}{\partial\nu}\left[\frac{J_{\nu-1}-J_{\nu+1}}{J_\nu}\right]$

* The prime corresponds to the derivative relative to the argument. The argument of the Bessel functions J and K are sw and δw, respectively. s and δ are the transverse wave vectors, and β are the longitudinal wave vectors of the unperturbed (smooth-boundary no-gain) waveguide. ν is the order of the Bessel function, d is the diffusion depth, and α is the change in the relative permittivity at the diffusion surface.

$$Y_{pq} = (\kappa_{pq}^2(k) + Y_{pq}^2(k))^{1/2} \coth (\kappa_{pq}^2(k) + Y_{pq}^2(k))^{1/2} L \tag{8}$$

where L is the length of the laser, c is the speed of light in vacuum, and ψ_i is the group velocity of the ith mode.

In Figs. 2 and 3, we plotted the coupling coefficient $\kappa_{pq}L$, the coefficient C, and the threshold gain GL as a function of the operating wavelength λ for a number of cases.

Near cutoff, the coupling coefficient is small because the optical energy is spread thinly over a large region. At high frequency, the coupling in the fiber case is again very weak because the energy is confined inside the core, and the field at the boundary is weak, thus explaining the increase–decrease behavior of $\kappa_{pq}L$. However, for the diffused guide, the energy tends to concentrate progressively more in the high-index region next to the corrugated boundary, thus giving a continuously increasing coupling coefficient. It should be mentioned that for very high frequency, when λ tends to become equal to η or smaller, our theory is not valid (Rayleigh limit).

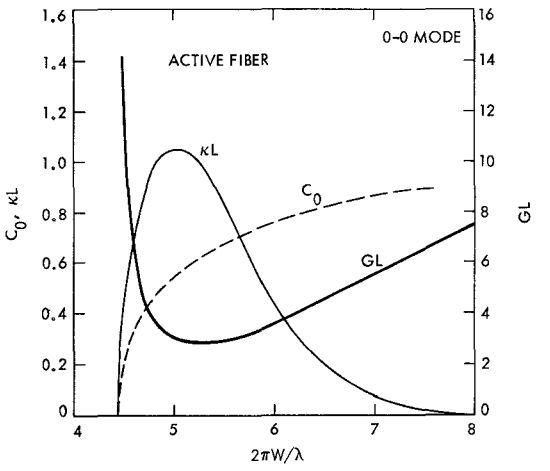

(a)

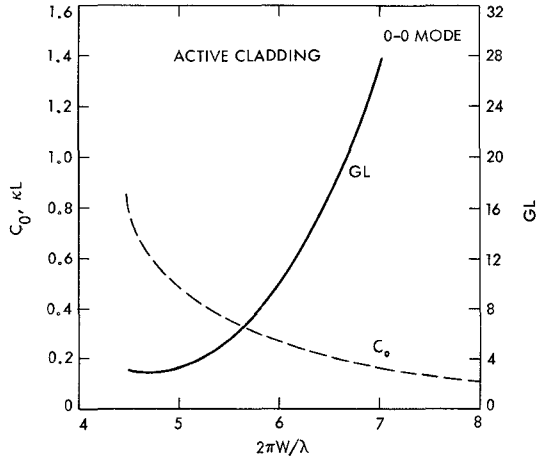

(b)

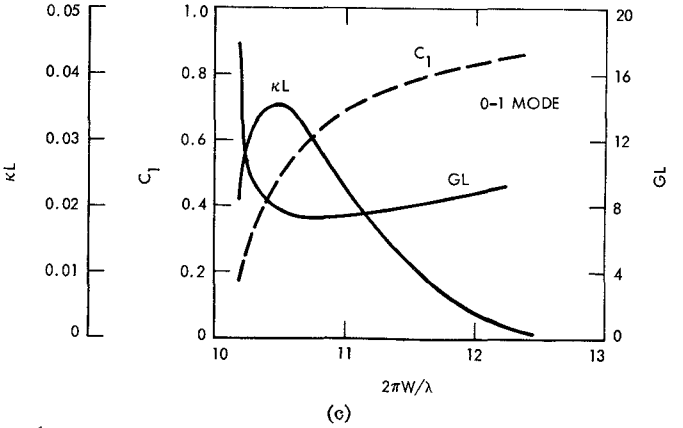

(c)

Fig. 2. Coupling coefficient, gain efficiency, and threshold gain coefficient for a DFB fiber laser. $\epsilon_1 = (1.5)^2$, $\epsilon_2 = (1.4)^2$. (a) 0–0 mode coupling with an active fiber. (b) 0–0 mode coupling with an active cladding. (c) 0–1 mode coupling with an active fiber. $\eta L/w^2 = 4$.

An interesting result of our calculations is that a fiber laser has an optimum operating region which requires the least gain for self-sustained oscillation. To illustrate, let us consider the case where: $D/2w = 0.01$, $\eta/w \simeq 6 \times 10^{-4}$, $L/a = 6600$, and $\lambda/w = 1.2$. For $\lambda = 1$ μm, this corresponds to $w = 0.83$ μm, $d = 0.016$ μm, and $L = 5.5$ mm. The corresponding threshold gain coefficients for the 0–0 coupling is $GL \simeq 3$ for an active fiber, and $GL \simeq 4.2$ for an active cladding. These gains could be achieved with some active materials (for instance, dye). A larger value of $D/2a$ would lead to even lower threshold gain.

In the case of a diffused waveguide, optimum operation occurs at the highest frequency possible. To illustrate, let us consider $\lambda = 0.63$ μm, $d = 1$ μm, $\eta = 0.015$ μm, and $L = 0.5$ cm. The threshold gain coefficient for an active diffused region is $GL = 0.4$ for the 0–0

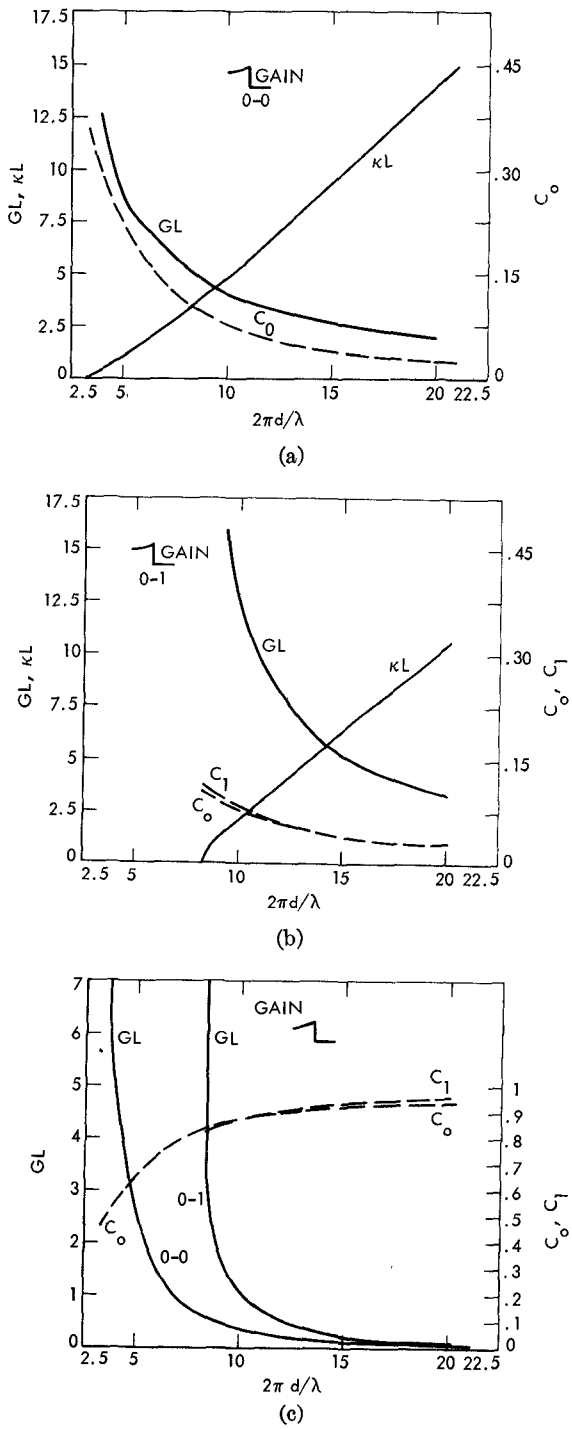

Fig. 3. Coupling coefficient, gain efficiency, and threshold gain coefficient for a DFB diffuse laser: $\epsilon_1 = (1.5)^2$, $\epsilon_2 = 1.0$, $\alpha = 0.1$. (a) 0–0 mode coupling. (b) 0–1 mode coupling with active homogeneous halfspace. (c) 0–0 and 0–1 mode coupling with active inhomogeneous halfspace. $\eta L/d^2 = 75$.

coupling, and $GL = 1.5$ for the 0–1 coupling. These gains are well below the limits of many active materials (dye, semiconductors).

In the case of a capillary guide [Fig. 1(c)], the threhsold gain for the case of an active channel is very close to the gain curve in Fig. 3(a).

Thus we conclude that fiber and diffuse waveguides can be effectively used to develop transversely bounded DFB lasers.

REFERENCES

[1] H. Kogelnik and C. V. Shank, *Appl. Phys. Lett.*, vol. 18, p. 152, 1971.
[2] K. O. Hill and A. Watanabe, *Opt. Commun.*, vol. 5, p. 289, 1972.
[3] D. P. Schinke, R. G. Smith, E. G. Spender, and M. F. Gavin, *Appl. Phys. Lett.*, vol. 21, p. 494, 1972.
[4] H. Kogelnik and C. V. Shank, *J. Appl. Phys.*, vol. 43, p. 2327, 1972.

[5] S. Wang, *J. Appl. Phys.*, vol. 44, p. 767, 1973.
[6] ——, "Principles of distributed feedback and distributed Bragg-reflector lasers," *IEEE J. Quantum Electron.*, vol. QE-10, pp. 413–427, Apr. 1974.
[7] D. Marcuse, "Hollow dielectric waveguide for distributed feedback lasers," *IEEE J. Quantum Electron.*, vol. QE-8, pp. 661–669, July 1972.
[8] R. Shubert, *J. Appl. Phys.*, vol. 45, p. 209, 1974.
[9] W. Chang, "Periodic structures and their application in integrated optics," *IEEE Trans. Microwave Theory Tech. (1973 Symposium Issue)*, vol. MTT-21, pp. 775–785, Dec. 1973.
[10] C. Elachi and C. Yeh, *J. Appl. Phys.*, vol. 44, p. 3146, 1973.
[11] C. Elachi, G. Evans, and C. Yeh, presented at the Integrated Optics Conf., New Orleans, La., Jan. 1974.
[12] H. F. Taylor, W. E. Martin, D. B. Hall, and V. N. Smiley, *Appl. Phys. Lett.*, vol. 21, p. 95, 1972.
[13] C. Elachi, G. Evans, and G. Franceshetti, *Alta Freq.*, vol. 43, p. 390, 1974.
[14] E. H. Conwell, *Appl. Phys. Lett.*, vol. 23, p. 328, 1973.
[15] D. Marcuse, *Light Transmission Optics*. New York: Van Nostrand-Reinhold, 1972.
[16] C. Elachi and C. Yeh, *J. Appl. Phys.*, vol. 45, p. 3494, 1974.

Letters

Comments on "Error in Impedance Measurement When the Signal is Introduced Across the Slotted-Line Probe"

ROBERT V. GARVER

In the above short paper,[1] an attempt was made to calculate the errors in VSWR and phase caused by detector mismatch in a backwards-connected (power into the probe) slotted line. The short paper is wrong. There will be no first-order errors as predicted theoretically in the referenced short paper. The errors encountered in measuring nonlinear devices (diodes) are more complex than those encountered in measuring linear devices. It is very important that the harmonics generated by the diode being measured be absorbed in a matched load and kept out of the detector (especially for high-VSWR diodes). A low-pass filter is commonly used in front of the detector, but (unless it is padded) this filter reflects the harmonic power back into the diode. When the diode being measured does not see a match at the harmonic frequencies, then the harmonic mismatch will interact with the diode to make more efficient or less efficient the conversion to harmonics, depending on the phase relationship between diode and harmonic mismatch. The variable conversion to harmonics will change the impedance of the diode being measured (at the fundamental frequency) as the phase between diode and harmonic mismatch (unpadded low-pass filter) is varied. Therefore, when using a backwards-connected slotted line, it is important to have in front of the detector a low-pass filter that is padded or otherwise matched at the harmonic frequencies as seen from the diode. It is not important for the detector to be matched at the fundamental frequency in a backwards-connected slotted line, as proven in the following discussion.

Generator mismatch causes no first-order errors when the generator is connected to a slotted line in the normal manner. Given a generator and detector with identical output (input) impedances, one can interchange them and there will be no change in energy transfer through the slotted-line network for a linear passive network. Therefore, detector mismatch causes no first-order errors in measurements using a backwards-connected slotted line when linear passive impedances are being measured.

The error made in the subject short paper is that the maximum and minimum of the standing wave between detector and unknown are calculated instead of the maximum and minimum voltage transfer from the generator to the real part of the detector impedance.

A simple experiment with a backwards-connected slotted line will prove the point. With the probe decoupled 30 dB and a good impedance match for an unknown, connect a detector with a 2:1 VSWR to the slotted-line input with a phase shifter between it and the slotted line. The VSWR of the good match will be measured for all settings of the phase shifter and not the VSWR of the detector.

As a mental experiment, take the case of a perfectly matched load for an unknown. In this case, the distance between detector and unknown will give no change in error. According to the subject

Manuscript received January 20, 1975.
The author is with the Harry Diamond Laboratories, Department of the Army, Adelphi, Md. 20783.
[1] J. Barbero, *IEEE Trans. Microwave Theory Tech.* (Short Papers), vol. MTT-22, pp. 887–889, Oct. 1974.